σ1-Receptor Agonism Protects against Renal Ischemia-Reperfusion Injury

Adam Hosszu,*† Zsuzsanna Antal,† Lilla Lenart,* Judit Hodrea,* Sandor Koszegi,* Dora B. Balogh,* Nora F. Banki,† Laszlo Wagner,‡ Adam Denes,§ Peter Hamar,‖ Peter Degrell,¶ Adam Vannay,** Attila J. Szabo,†** and Andrea Fekete*†

*MTA-SE Lendulet Diabetes Research Group and **MTA-SE Pediatrics and Nephrology Research Group, Hungarian Academy of Sciences and Semmelweis University, Budapest, Hungary; †First Department of Pediatrics, ‡Department of Transplantation and Surgery, and ‖Institute of Pathophysiology, Semmelweis University, Budapest, Hungary; §Laboratory of Neuroimmunology, Institute of Experimental Medicine, Budapest, Hungary; and ¶Department of Pathology, Moritz Kaposi General Hospital, Kaposvar, Hungary

ABSTRACT

Mechanisms of renal ischemia-reperfusion injury remain unresolved, and effective therapies are lacking. We previously showed that dehydroepiandrosterone protects against renal ischemia-reperfusion injury in male rats. Here, we investigated the potential role of σ1-receptor activation in mediating this protection. In rats, pretreatment with either dehydroepiandrosterone or fluvoxamine, a high–affinity σ1–receptor agonist, improved survival, renal function and structure, and the inflammatory response after sublethal renal ischemia-reperfusion injury. In human proximal tubular epithelial cells, stimulation by fluvoxamine or oxidative stress caused the σ1-receptor to translocate from the endoplasmic reticulum to the cytosol and nucleus. Fluvoxamine stimulation in these cells also activated nitric oxide production that was blocked by σ1-receptor knockdown or Akt inhibition. Similarly, in the postischemic rat kidney, σ1-receptor activation by fluvoxamine triggered the Akt-nitric oxide synthase signaling pathway, resulting in time– and isoform–specific endothelial and neuronal nitric oxide synthase activation and nitric oxide production. Concurrently, intravital two–photon imaging revealed prompt peritubular vasodilation after fluvoxamine treatment, which was blocked by the σ1-receptor antagonist or various nitric oxide synthase blockers. In conclusion, in this rat model of ischemia-reperfusion injury, σ1-receptor agonists improved postischemic survival and renal function *via* activation of Akt–mediated nitric oxide signaling in the kidney. Thus, σ1-receptor activation might provide a therapeutic option for renoprotective therapy.

J Am Soc Nephrol 28: 152–165, 2017. doi: 10.1681/ASN.2015070772

Renal ischemia-reperfusion injury (IRI) –induced AKI occurs during several clinical conditions, and it is the main cause of delayed graft function or graft loss after kidney transplantation.[1] Despite improvements in therapy, IRI is still associated with unacceptably high mortality of up to 79%[2]; therefore, new treatment approaches are urgently needed.

Endothelial dysfunction, peritubular capillary loss, and increased reactivity to vasoconstrictive agents are all known prominent features of tubular damage during the progression of IRI. All of these processes contribute to decreased production and impaired responsiveness to nitric oxide (NO).

We previously proved that sex hormones have a strong influence on the outcome of IRI; female rats live longer, have less impaired postischemic renal function, and have milder structural damage than males.[3–5] Furthermore, we showed that female rats have lower

Received July 16, 2015. Accepted March 5, 2016.

Published online ahead of print. Publication date available at www.jasn.org.

Correspondence: Dr. Andrea Fekete, First Department of Pediatrics, Semmelweis University, Bókay János u. 53-54, 1083 Budapest, Hungary. Email: fekete.andrea@med.semmelweis-univ.hu

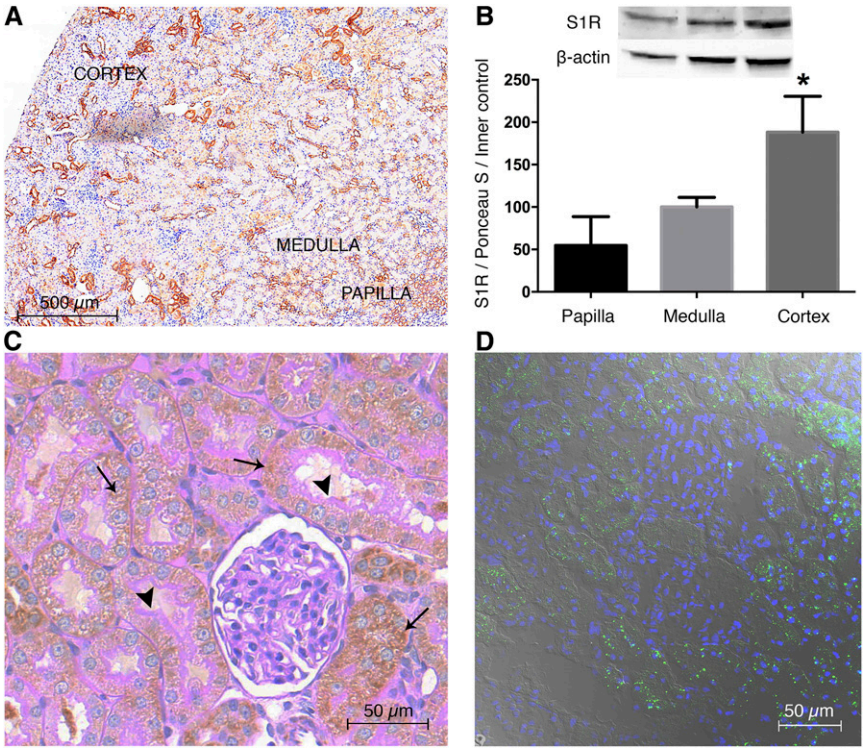

Figure 1. S1R is predominantly expressed in the renal cortex. (A) Representative rat kidney section stained with anti-S1R (brown; 6× DAB). Scale bar, 500 μm. (B) Immunoblot for renal S1R. S1R is expressed in the papilla, medulla, and most prominently, the cortex. Representative blots are shown. Bars indicate means±SEMs; data were analyzed by one-way ANOVA with Bonferroni multiple comparison test. *$P<0.05$ versus papilla and medulla ($n=6$ per group). (C) Representative kidney section developed with peroxidase anti-S1R (brown) and counterstained with PAS (pink). Thin black arrows show S1R in proximal tubules but not in glomerulus. Black arrowheads point to intact, PAS–stained brush borders of proximal tubules. Scale bar, 50 μm. (D) Representative image of fluorescent immunohistochemistry double staining of rat kidney for nuclei (blue) and S1R (green). Scale bar, 50 μm.

endothelin expression[4] but higher nitric oxide synthase enzyme (NOS) levels,[6,7] suggesting that sex hormones play a significant role in the regulation of endothelium-derived NO during IRI.

Recently, we showed that dehydroepiandrosterone (DHEA) is protective against renal IRI in male rats[8]; however, this protection seemed to be independent of the estrogenic effect of DHEA. Studies indicate that various receptors of DHEA are expressed in the plasma membrane, where DHEA activates Akt and endothelial nitric oxide synthase enzyme (eNOS) signaling pathways.[9] One of these receptors is the σ1-receptor (S1R).

S1R is a highly conserved protein that is mainly present in the brain[10] and also expressed in peripheral tissues, including the kidney.[11,12] However, its renal function and regulation still remain elusive. Fluvoxamine (FLU) is a potent selective S1R agonist with an affinity 1000-fold higher than DHEA.[13] Recently, it has been shown that FLU ameliorates ischemic cardiac[14,15] and brain damage,[16] although its potential effect on renal postischemic injury has not been elucidated yet. Moreover, the direct effects of S1R activation on renal tubular cells have not been described at all.

In this preclinical study, we examined the effects of S1R agonism in a model of IRI-induced AKI with impaired Akt-NOS signaling. We found that DHEA and FLU effectively prevent renal IRI, suggesting that S1R agonism might have novel therapeutic potential in the treatment of AKI.

RESULTS

S1R Expression in the Kidney

First, we wanted to assess whether S1R is indeed localized in the kidney. As shown by 3,3′-diaminobenzidine (DAB) staining, fluorescent immunohistochemistry and Western blot S1R expression were most prominent in the renal cortex but also present in the medulla and papilla (Figure 1, A and B).

The next step was to prove that S1R is localized in the proximal tubules. Costaining kidney sections with brush border membrane–specific periodic acid–Schiff (PAS) and anti–S1R DAB revealed that S1R is definitely expressed in proximal tubules but not in glomeruli (Figure 1C).

DHEA Prolongs Survival, Improves Kidney Function, and Ameliorates Structural Damage after Renal IRI

To determine the S1R-mediated effect of DHEA, rats received vehicle (ischemia-reperfusion [I/R]) or DHEA treatment (I/R DHEA) and were subjected to 50 minutes of renal IRI.

DHEA-treated rats survived longer than vehicle-treated ones (median survival: 72 versus 36 hours; $P<0.001$). One third of I/R DHEA rats completely recovered, whereas all I/R animals died within 75 hours (Figure 2A).

To investigate the acute effects of IRI, one series of animals was harvested 24 hours after IRI. BUN and creatinine levels increased in all groups, showing postischemic AKI (Figure 2, B and C). Histologic changes were consistent with functional deterioration. Intravital microscopy showed postischemic vasoconstriction (Figure 2D), suggesting that the subsequent decline in renal blood flow could be a causative factor of renal functional and structural damage. Twenty-four hours after IRI, >75% of tubules showed cell necrosis, no brush border was visible, and cast formation was extensive in vehicle-treated rats (Figure 2F).

DHEA pretreatment (T24 I/R DHEA) prevented peritubular vasoconstriction, markedly inhibited cell necrosis, and

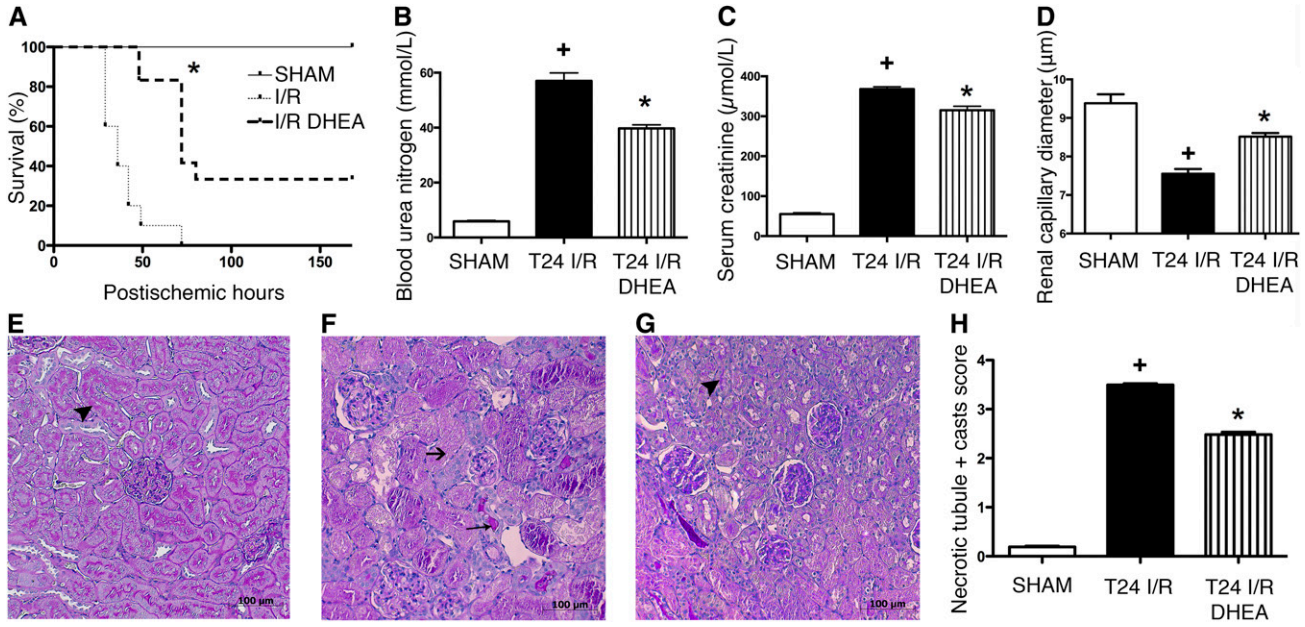

Figure 2. DHEA pretreatment is protective against renal IRI. (A) Postischemic survival was followed for 7 days in rats pretreated with vehicle (I/R) or DHEA (I/R DHEA) 25 and 1 hour before the 50-minute ischemia. Log rank test (n=8 per group). *P<0.001 versus I/R. (B) BUN levels of vehicle (T24 I/R) and DHEA (T24 I/R DHEA) -pretreated rats after 24 hours of reperfusion. *P<0.05 versus T24 I/R (n=6 per group); ^{+}P<0.05 versus sham (n=6 per group). (C) Serum creatinine levels. *P<0.05 versus T24 I/R (n=6 per group); ^{+}P<0.05 versus sham (n=6 per group). (D) Renal capillary diameters measured using intravital two–photon microscopy. Approximately 150 capillaries per animal. Bars indicate means±SEMs, and data were analyzed by one-way ANOVA with Bonferroni multiple comparison test. *P<0.05 versus T24 I/R (n=3 per group); ^{+}P<0.05 versus sham (n=3 per group). (E–G) Representative images of structural damage after IRI on PAS–stained kidney sections of (E) sham-operated, (F) T24 I/R, or (G) T24 I/R DHEA–pretreated rats. Black arrowheads points to intact brush border, long thin black arrow shows hyaline accumulation, and short black arrow shows necrotic tubule. Original magnification, ×200. (H) Semiquantitative evaluation of tubular injury on a zero to four scale. Bars indicate medians ± ranges, and data were analyzed by Kruskal–Wallis test with Dunn correction. *P<0.05 versus T24 I/R (n=6 per group); ^{+}P<0.05 versus sham (n=6 per group).

preserved tubular brush border membrane (Figure 2, E–H), pointing to a possible S1R–mediated renal protection after IRI.

FLU Pretreatment Improves Survival as well as Kidney Function after Renal IRI

To further prove the crucial role of S1R in IRI, we proceeded with the much higher affinity agonist FLU. FLU-treated rats (I/R F) survived longer than vehicle (I/R) or FLU- and *N*,*N*-dipropyl-2-[4-methoxy-3-(2-phenylethoxy)-phenyl]-ethylamine monohydrochloride (NE100) –treated (a selective S1R antagonist) ones (I/R FN; median survival: 67 versus 36 or 49 hours, respectively; P<0.001). One third of I/R F rats recovered completely, whereas all I/R and I/R FN animals died within 70 hours (Figure 2A). FLU improved renal function, because creatinine and BUN levels were almost recovered by 168 hours in the FLU-treated survivors (I/R F) (Figure 3, B and C). Aspartate aminotransferase (AST) is also regarded as a marker of renal tubular damage, and elevated levels of AST after renal IRI decreased to normal after FLU treatment (Figure 3D).

These parameters were also less elevated in FLU-treated rats after 24 hours of reperfusion (T24 I/R F). The improvement was diminished by NE100 (T24 I/R FN).

Hypoxia–inducible factor–α (HIF-1α) mediates cell protection and epithelium recovery after renal IRI.[17] Hif-1α mRNA expression increased as soon as 2 hours after ischemia (T2 I/R), and the increase was even stronger in FLU-treated (T2 I/R F) rats (Figure 3E). Neutrophil gelatinase–associated lipocalin (NGAL) is a specific indicator of kidney injury that correlates with the severity of renal impairment.[18] A robust elevation in Ngal mRNA expression was seen after 24 hours of reperfusion (T24 I/R), but the increase was milder in FLU-treated (T24 I/R F) rats (Figure 3F). Proximal tubular injury marker Kidney Injury Molecule-1 (KIM-1)[19] was upregulated in the postischemic kidney. Increased Kim-1 mRNA expression was ameliorated by FLU (T24 I/R F), which also suggests milder proximal tubular damage (Figure 3G).

FLU Attenuates IRI-Induced Inflammation

IRI–induced systemic inflammation was represented by elevated serum white blood cell count and increased level of renal inflammatory cytokines (IL-1α, TNF-α, and IL-6). FLU treatment reduced white blood cell count by 30% (T24 I/R F: 4.36±0.52×10^9/L versus T24 I/R: 6.23±0.76×10^9/L and T24 I/R FN: 6.21±0.58×10^9/L; P<0.05). IL-1α and IL-6 levels were reduced by 70% and 80%, respectively, whereas anti–inflammatory cytokine IL-10 was increased by 15% (Table 1).

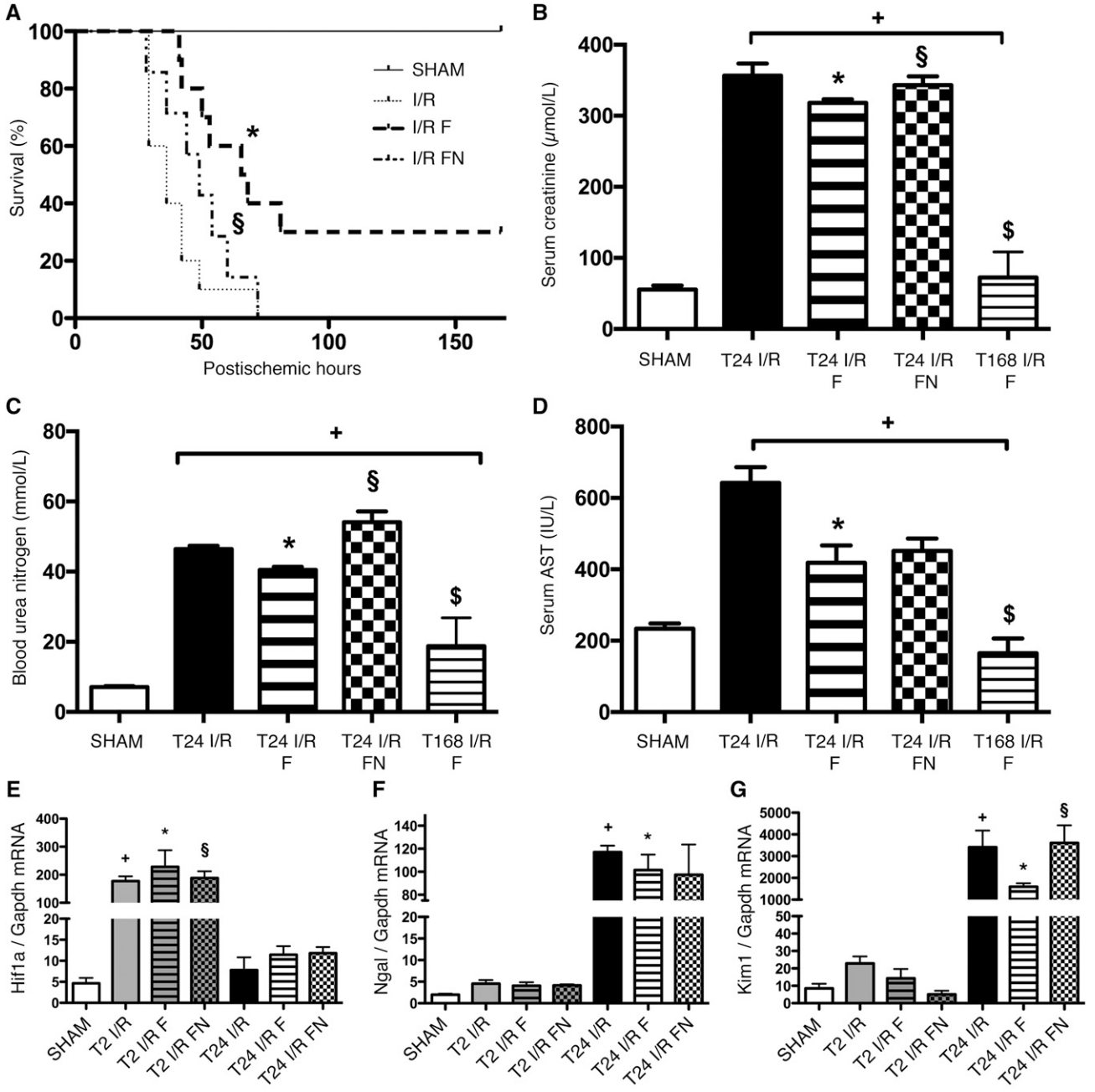

Figure 3. FLU pretreatment is protective against renal IRI. (A) Rats were pretreated with isotonic saline (I/R), FLU (I/R F), or FLU and NE100 (I/R FN) 30 minutes before the 50-minute ischemia. Postischemic survival was followed for 7 days. Log rank test (n=8 per group). *P<0.001 versus I/R; $^{\S}P$<0.001 versus I/R F. (B) Serum creatinine levels after 24 hours of reperfusion in FLU-treated (T24 I/R F) and FLU + NE100–treated (T24 I/R FN) rats and after 168 hours of reperfusion in FLU-treated (T168 I/R F) rats. *P<0.05 versus T24 I/R (n=8 per group); ^{+}P<0.05 versus sham (n=8 per group); $^{\S}P$<0.05 versus T24 I/R F (n=8 per group); $^{\$}P$<0.05 versus T24 I/R ($n$=8 per group). (C) BUN levels. *P<0.05 versus T24 I/R (n=8 per group); ^{+}P<0.05 versus sham (n=8 per group); $^{\S}P$<0.05 versus T24 I/R F (n=8 per group); $^{\$}P$<0.05 versus T24 I/R ($n$=8 per group). (D) Serum AST levels. *P<0.05 versus T24 I/R (n=8 per group); ^{+}P<0.05 versus sham (n=8 per group); $^{\$}P$<0.05 versus T24 I/R ($n$=8 per group).(E) Renal Hif-1α mRNA expression normalized to glyceraldehyde-3-phosphate dehydrogenase (Gapdh) expression. *P<0.05 versus T24 I/R (n=6 per group); ^{+}P<0.05 versus sham (n=6 per group); $^{\S}P$<0.05 versus T24 I/R F (n=6 per group). (F) Renal Ngal mRNA expression normalized to Gapdh expression. *P<0.05 versus T24 I/R (n=6 per group); ^{+}P<0.05 versus sham (n=6 per group). (G) Renal Kim-1 mRNA expression normalized to Gapdh expression. Bars indicate means±SEMs, and data were analyzed by one-way ANOVA with Bonferroni multiple comparison test. *P<0.05 versus T24 I/R (n=6 per group); ^{+}P<0.05 versus sham (n=6 per group); $^{\S}P$<0.05 versus T24 I/R F (n=6 per group).

FLU Ameliorates Renal Structural Damage after IRI

IRI–induced histologic injury was assessed in PAS–stained kidney sections. Severe structural damage was characteristic to IRI: leukocyte infiltration and hyaline accumulation were prevalent, and brush borders were severely damaged, suggesting loss of function as well as structural damage (Figure 4, D and E). In T24 I/R F rats, however, tubular damage and cell necrosis were only moderate, and brush borders were intact in several regions (Figure 4B). In the FLU-treated rats that survived the 168 hours of the postischemic period, tubular damage was abolished: cell necrosis was scarcely visible, and brush borders were recovered almost everywhere (Figure 4C).

Intravital two–photon microscopic imaging revealed similar renal structure. Brush border membrane was intact in several areas in T24 I/R F rats, indicating that FLU preserved renal function, whereas no brush border was visible in the cortex of either T24 I/R or T24 I/R FN animals. In the T24 I/R F group, nuclei were intact, and necrotic cast formation was minimal as opposed to severe cell necrosis and cast formation in T24 I/R and T24 I/R FN groups (Figure 5).

S1R in the Ischemic Kidney

Anti–S1R DAB staining was more intensive already after I/R but most prominent after FLU treatment, suggesting a higher S1R production in this group (Figure 6, A–D). This is in line with increased S1R protein levels measured by Western blot (Figure 6I). Fluorescence staining on high magnification (×630) showed a predominantly perinuclear ring–like S1R staining pattern in the renal proximal tubular epithelium of shams. After I/R and FLU treatment, S1R staining was visible in the whole cytoplasm, and intranuclear localization was also detectable (Figure 6, E–H).

FLU Induces S1R–Mediated NO Production in HK2 Cells

To our best knowledge, this is the first report showing that S1R is expressed in human proximal tubular epithelial cells. S1R expression was not upregulated by either FLU or H_2O_2 treatment in tubular cells (Figure 7A); however, its localization was different under normal conditions and after oxidative stress. After S1R showed a perinuclear localization in control cells (C), the receptor was detected everywhere intracellularly and also, in the nucleus after H_2O_2 or FLU (F) treatment (Figure 7, B–D).

Cellular fractionation confirmed that, although the abundance of S1R remains unaltered, on stimulation, it translocates from the ER to the cytosol and/or nucleus (Figure 6, F and G) and might activate signaling pathways.

FLU increased phospho-endothelial nitric oxide synthase enzyme (peNOS; Ser1177) protein levels in tubular cells under both normal conditions (F) and oxidative stress (H_2O_2 F). The S1R antagonist NE100 neutralized this increase (FN; H_2O_2 FN) (Figure 7H). Neuronal nitric oxide synthase enzyme (nNOS) was not detectable in proximal tubular cells in any of the groups.

The direct role of S1R in eNOS production was proven by S1R knockdown as well. Parallel with a 70% decrease in S1R protein level, peNOS levels were also lower compared with scrambled siRNA–treated negative controls. Decreased peNOS production in FLU–treated S1R knockdown cells (S1R siRNA F) verified the regulatory role of S1R in peNOS expression (Figure 7, I and J).

To validate the role of Akt in FLU–induced NOS activation and NO production, various Akt inhibitors were used to suppress both the upstream (Akt IV) and downstream (Akt VIII) activation and/or phosphorylation of Akt. Inhibition of Akt suppressed peNOS and subsequently, NO production in FLU-treated cells (Figure 7, K and L).

FLU Induces S1R–Mediated Vasodilative NOS Production in the Rat Kidney

To investigate the vasoregulatory effect of FLU, peritubular capillary diameters were measured by intravital two–photon microscopy in sham-operated rats after 30 minutes of FLU treatment. Parallel with increased peNOS expression (Figure 8E) and NO production (Figure 8C), FLU pretreatment (T30' F) increased peritubular capillary diameters. The addition of nonselective NOS blocker *N*-ω-Nitro-L-arginine methyl ester (T30' F + NAME), selective nNOS blocker 7-Nitroindazole (T30' F + 7-NI), and most prominently, selective eNOS blocker *N*-5-(1-Iminoethyl)-L-ornithine dihydrochloride inhibited FLU-mediated vasodilation (Figure 8A).

Parallel with increased nitrite concentration (Figure 8C), significant peritubular capillary dilation was detected in FLU-treated rats after 24 hours of reperfusion (T24 I/R F) as well, which was diminished by NE100 (T24 I/R FN) or various NOS blockers, supporting that the vasodilative effect of FLU is S1R mediated and NOS dependent (Figure 8B, Supplemental Figures 3 and 4).

To evaluate the effect of FLU on the S1R signaling pathway, S1R, pAkt (Ser473), peNOS (Ser1177), and nNOS protein levels were measured 30 minutes after FLU treatment in sham-operated (T30' F) rats and at T24 after IRI. FLU increased pAkt and peNOS protein levels as soon as 30 minutes after treatment, whereas S1R and nNOS remained unchanged (Figure 8, D–F). However, after 24 hours of reperfusion (T24 I/R F), S1R, peNOS and nNOS were upregulated, suggesting that, although

Table 1. Renal cytokine levels

Cytokine	Sham	T24 I/R	T24 I/R F	T24 I/R FN
IL-1α, pg/ml	0.17±0.16	58.7±16.3[a]	16.1±4.82[b]	11.4±6.33
IL-6, pg/ml	0.00±0.00	141±14.9[a]	29.6±3.36[b]	32.4±10.4
TNF-α, pg/ml	106±2.07	138±16.4	149±8.67	135±8.76
IL-10, pg/ml	75.6±1.61	98.0±5.87[a]	113±7.95[b]	86.6±2.54[c]
IL-4, pg/ml	8.74±1.11	9.88±0.80	10.6±0.11	10.1±0.15

Cytokine levels were measured from renal tissue homogenates by cytometric bead array. Kidney tissues were collected after 24 hours of reperfusion from vehicle (T24 I/R), FLU (T24 I/R F), or FLU + NE100 (T24 I/R FN) –treated rats (n=6 per group). Values indicate means±SEMs, and data were analyzed by one-way ANOVA with Bonferroni multiple comparison test.
[a] $P<0.05$ versus sham.
[b] $P<0.05$ versus T24 I/R.
[c] $P<0.05$ versus T24 I/R F.

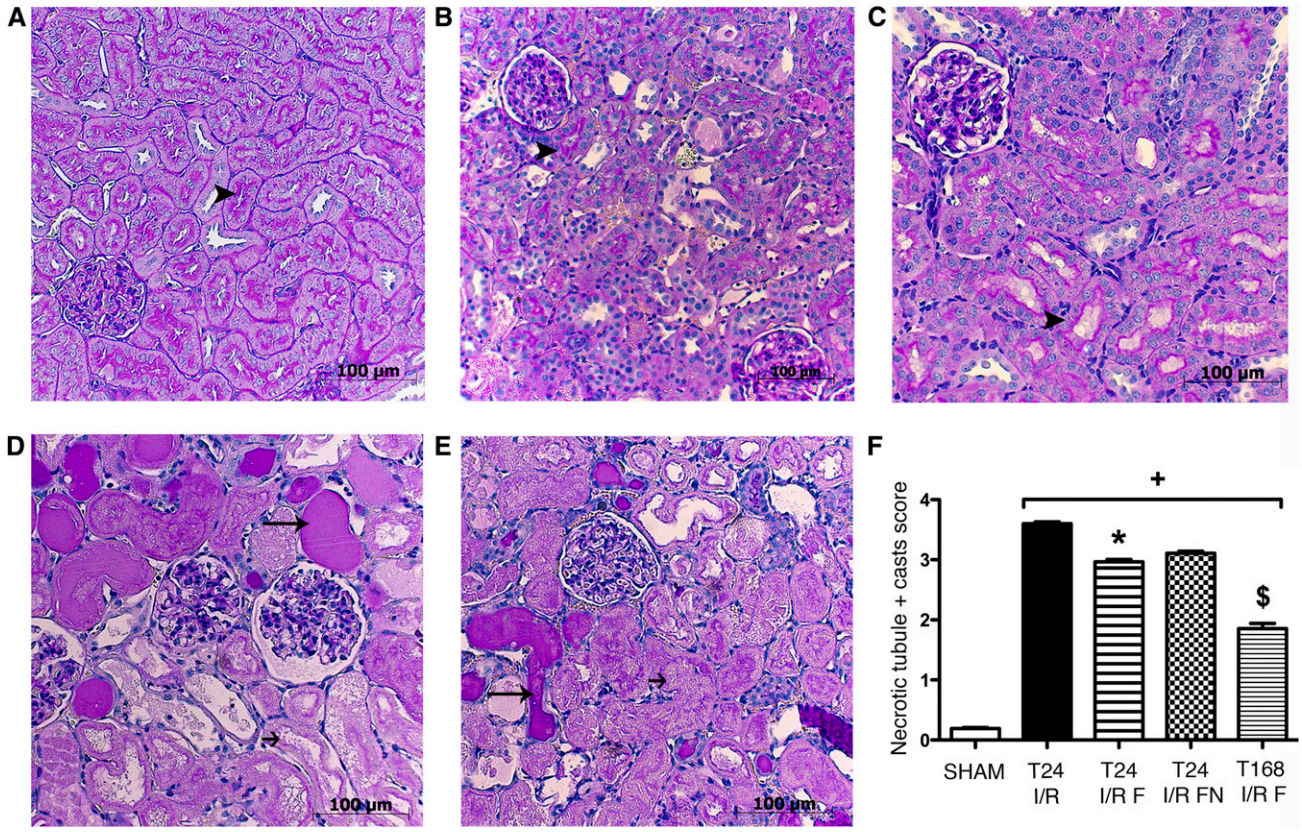

Figure 4. FLU ameliorates renal structural damage. (A–E) Representative PAS–stained kidney sections of (A) sham-operated, (B) T24 I/R F, (C) T168 I/R F, (D) T24 I/R, and (E) T24 I/R FN rats. Black arrowheads point to intact brush border, long thin black arrows show hyaline accumulation, and short black arrows show necrotic tubule. Original magnification, ×200. Scale bar, 100 μm. (F) Semiquantitative evaluation of tubular injury on a zero to four scale. Bars indicate medians ± ranges, and data were analyzed by Kruskal–Wallis test with Dunn correction. *$P<0.05$ versus T24 I/R ($n=6$ per group); $^{+}P<0.05$ versus sham ($n=6$ per group); $^{\$}P<0.05$ versus T24 I/R ($n=6$ per group).

peNOS production is instantaneous after S1R stimulation, nNOS generation increases later during reperfusion (Figure 8, E and F). As a result of increased NOS abundance, NO production was also considerably increased, contributing to the vasodilation. (Figure 8C).

DISCUSSION

Our study is the first to show that S1R agonism is protective in renal IRI essentially by improving postischemic survival and renal function and ameliorating renal structural damage. In fact, 1 week after the ischemic insult, renal function returned to almost normal, and kidney histology was similar to that of healthy rats. We detected, for the first time, S1R in proximal tubular cells and proved its direct effect on NO production. Furthermore, we showed *in vivo* that the activation of S1R leads to NO-mediated vasodilation and has a beneficial effect on renal perfusion.

On the basis of our first series of experiments, we speculated that S1R activation by DHEA is renoprotective in AKI by improving NO–mediated kidney perfusion. To further prove the crucial role of S1R in IRI, in a second series, we proceeded with the exogenous agonist FLU, which has a much higher affinity to S1R than DHEA (K_i FLU =36 nM versus K_i DHEA<10 μM).[13]

The protective effect of FLU was substantiated by a robust improvement in postischemic survival. In fact, the FLU-treated group was the only one where 30% of the animals survived the 1-week period and completely recovered from the ischemic insult. Several clinical studies show that, during/after AKI, even a minimal increase in serum creatinine is associated with increased mortality,[20,21] which is in line with our study, where a 13% acute improvement in renal function was coupled with substantial improvement in survival.

Recent papers widely discuss that serum creatinine and BUN are suboptimal markers of AKI. Therefore, we measured several other sensitive and early markers, which were all upregulated after IRI. Serum AST, renal Ngal and the proximal tubule–specific Kim-1[18,19] were considerably less elevated after FLU treatment, which also confirmed milder renal injury.

HIF-1α is not only a kidney injury marker, but also, it mediates cell protection and tubular recovery during renal

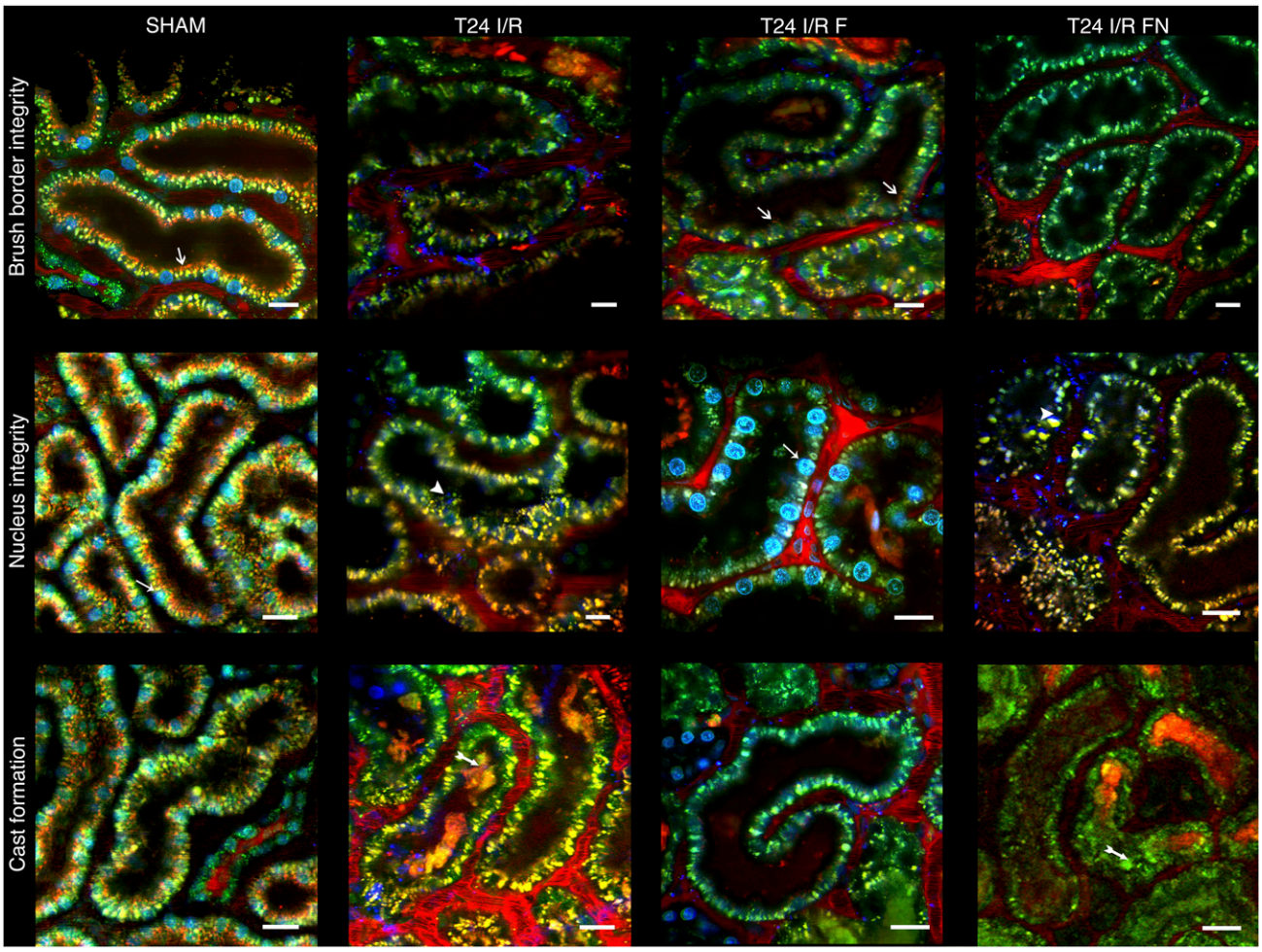

Figure 5. FLU ameliorates postischemic renal cortical damage. Representative intravital two–photon images of the rat kidney after 24 hours of reperfusion (T24 I/R) with FLU (T24 I/R F) or FLU and NE100 (T24 I/R FN) pretreatment. Brush border integrity is shown in top panel. White arrows show orange–colored Texas Red staining of intact brush borders. Nucleus integrity is shown in middle panel. Nuclei stained with Hoechst 33342 appear in blue. Thin white arrows point to intact nuclei. White arrowheads show severely damaged, disintegrated nuclei. In bottom row, two–tailed white arrows show extensive necrotic cast formation (n=3 per group). Scale bar, 25 μm.

IRI.[17] Numerous reports indicate that Akt is involved in the regulation of HIF-1α expression,[22,23] and because we found that S1R activation induces Akt phosphorylation, we suspect that Akt could be one link between S1R and HIF-1α.

Both conventional histology and intravital two–photon imaging revealed that FLU blunted the development of tubular damage. One week after FLU treatment, kidney structure was almost completely amended, and only remote leukocyte infiltration pointed to ceased inflammation.

Cytokine profile of the kidney verified a depressed inflammatory response as well. IL-1α has been recently identified as an early proinflammatory mediator in cerebral ischemia and a key driver of cerebrovascular inflammation[24,25]; however, its role in renal IRI has not been investigated yet. Here, we found that IL-1α levels were less elevated in rats receiving FLU pretreatment, whereas the powerful regulatory cytokine IL-10 was increased by FLU. IL-10 can block proinflammatory processes and inhibit leukocyte activation. In mice, administration of IL-10 prevented kidney injury.[26] We hypothesize that inflammatory response could be highly regulated by IL-10 in FLU-treated rats as opposed to vehicle-treated ones, in which we detected a more robust increase in proinflammatory cytokine levels (TNF-α, IL-1α, and IL-6) with less regulation associated with worse outcome. AKI is known to cause multiorgan dysfunction (heart, brain, and lungs) *via* systemic inflammation.[27] In models of brain and heart ischemia, the protective effect of S1R agonists has partly been attributed to their anti-inflammatory actions.[15,28] Therefore, it is plausible that, alongside renoprotection, the systemic anti–inflammatory actions of FLU also contribute to better outcomes in our study.

The proximal tubular epithelium is particularly sensitive to IRI, making it a potential therapeutic target. We were the first to detect S1R in these cells. S1R is localized in the ER membrane but can translocate to the plasma membrane.[29] On ligand stimulation or ER stress, S1Rs dissociate from binding Ig

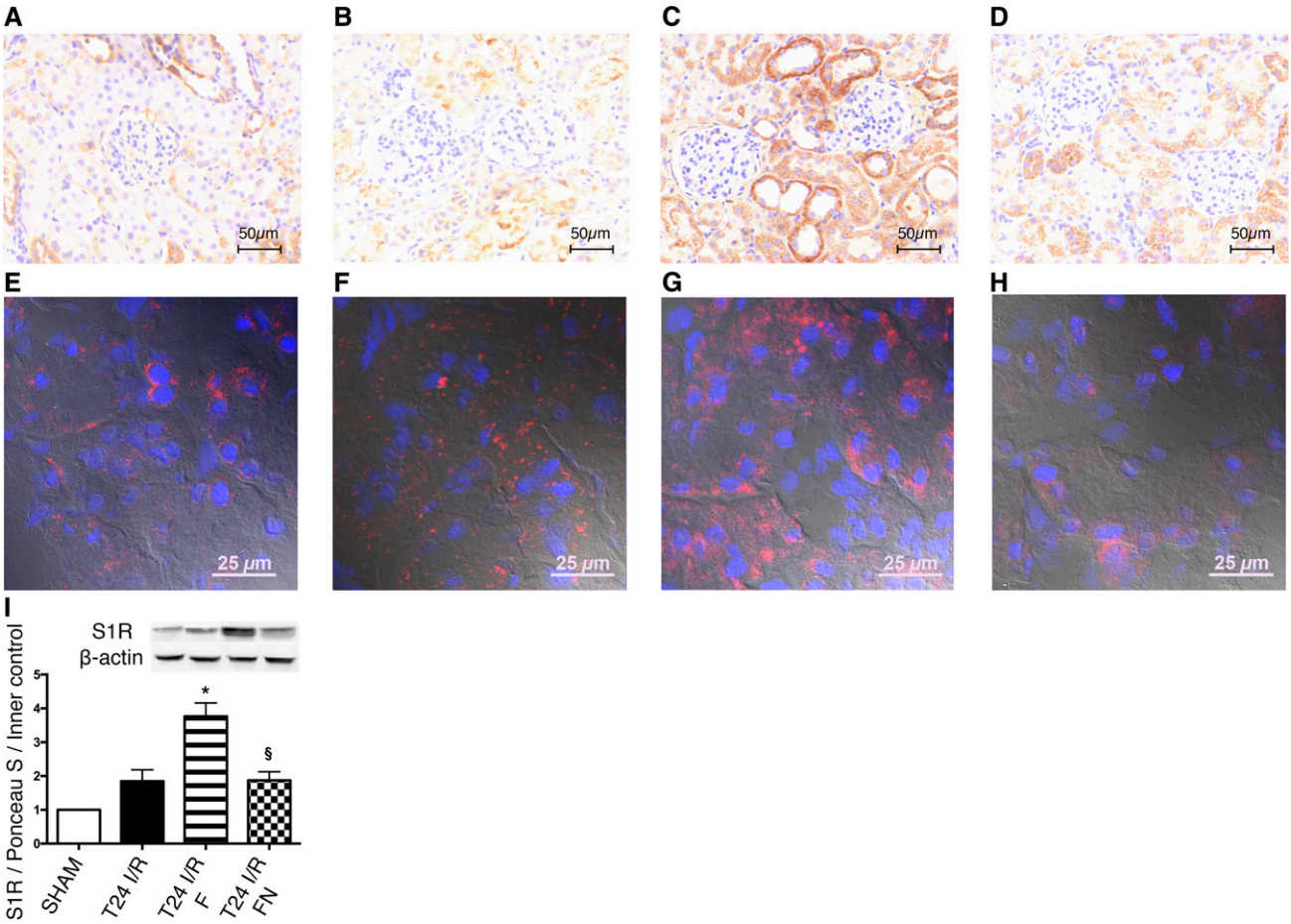

Figure 6. S1R translocates after renal I/R and FLU treatment. (A–D) Representative anti–S1R DAB–stained kidney sections of (A) sham-operated, (B) T24 I/R, (C) T24 I/R F, and (D) T24 I/R FN rats. Scale bar, 50 μm. (E–H) Representative immunohistochemical double–stained kidney sections for nuclei (blue) and S1R (red) of (E) sham-operated, (F) T24 I/R, (G) T24 I/R F, and (H) T24 I/R FN rats. Scale bar, 25 μm. (I) Immunoblot for renal S1R expression. Representative blots are shown. Bars indicate means±SEMs, and data were analyzed by one-way ANOVA with Bonferroni multiple comparison test. *$P<0.05$ versus T24 I/R (n=5–7 per group); §$P<0.05$ versus T24 I/R F (n=5–7 per group).

protein and act as interorganelle signaling modulators.[30] Congruently, we observed a perinuclear pattern of S1R in proximal tubular epithelial cells under normal conditions, but the receptor was expressed everywhere in the cytosol and nucleus after FLU treatment or under H_2O_2–induced oxidative stress. It is conceivable that S1Rs on translocating from the ER induce inositol requiring 1 protein kinase, which in turn, contributes to PI3K/Akt phosphorylation and activation.[31]

To determine the effect of FLU–mediated NOS production on renal perfusion, we measured peritubular capillary diameters in the live kidney. Evidence for active control of capillary diameter by pericytes in response to vasoactive molecules, such as NO, has already been shown.[32,33] Indeed, in line with increased NO production, vasodilation was apparent within minutes after FLU treatment. Similarly, IRI-induced vasoconstriction was reversed by FLU. Vasodilation did not occur if either S1R antagonist or NOS inhibitors was administered together with FLU, validating the hypothesis that S1R activation enhances NO production in the kidney and results in better blood supply, which leads to milder ischemic injury.

There is a general agreement that the macula densa is the principle site of nNOS production in the kidney, but a smaller amount is also present in proximal and distal tubules.[34] Here, we detected prompt eNOS production after S1R stimulation, whereas nNOS was elevated only later during reperfusion. This is congruent with an earlier study, where eNOS activity peaked 2 hours after reperfusion and returned to baseline after 3 days,[35] and it confirms our previous results in a different renal disease model showing that eNOS and nNOS have different expression patterns in time.[36]

It is worth considering that FLU is mainly used as a selective serotonin reuptake inhibitor (SSRI) in the chronic management of depression. SSRIs can also influence the serotonergic and noradrenergic systems in the brain; therefore, their role cannot be fully ruled out. However, it has already been proven in the heart and brain that paroxetine, an SSRI with very low affinity to S1R, was unable to produce the same protective effects as FLU.[15,37]

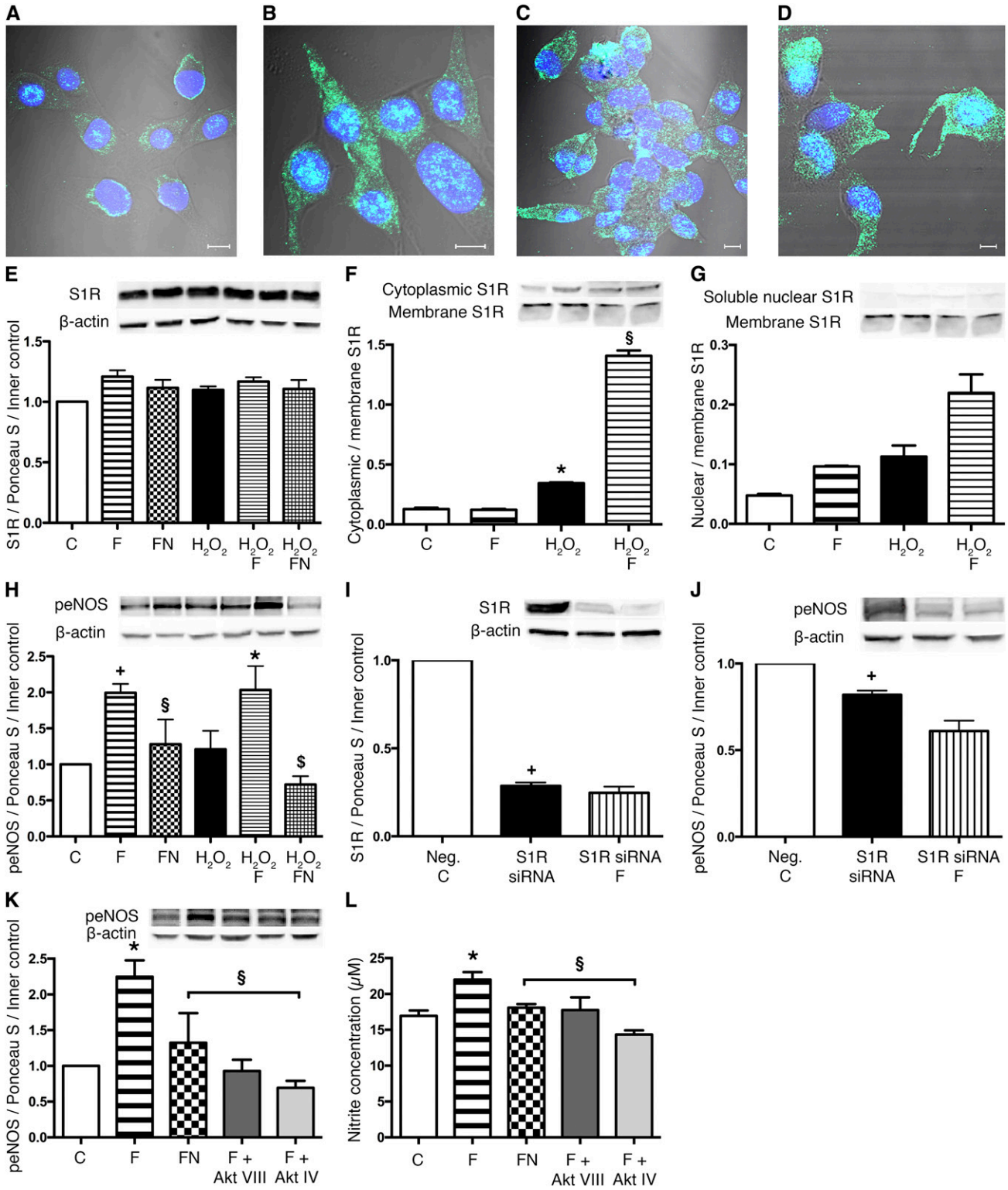

Figure 7. S1R translocates to the cytoplasm and nucleus after ligand stimulation and oxidative stress. (A–D) Representative images of fluorescent immunohistochemistry double staining of (A) control, (B) H_2O_2 (C) FLU, and (D) H_2O_2 and FLU–treated HK2 cells. Nuclei (blue) and anti-S1R (green). Scale bar, 5 μm. (E) Immunoblot for S1R protein in HK2 cells after FLU (F), FLU + NE100 (FN), H_2O_2, H_2O_2 + FLU (H_2O_2 F), and H_2O_2 + FLU + NE100 (H_2O_2 FN) treatment compared with untreated control (C) cells (n=6 per group). (F) Cytoplasmic-to-membrane ratio of S1R in HK2 cells after various treatments. Representative blots are shown. *P<0.05 versus C (n=5 per group); §P<0.05 versus H_2O_2 (n=5 per group). (G) Nuclear-to-membrane ratio of S1R in HK2 cells after various

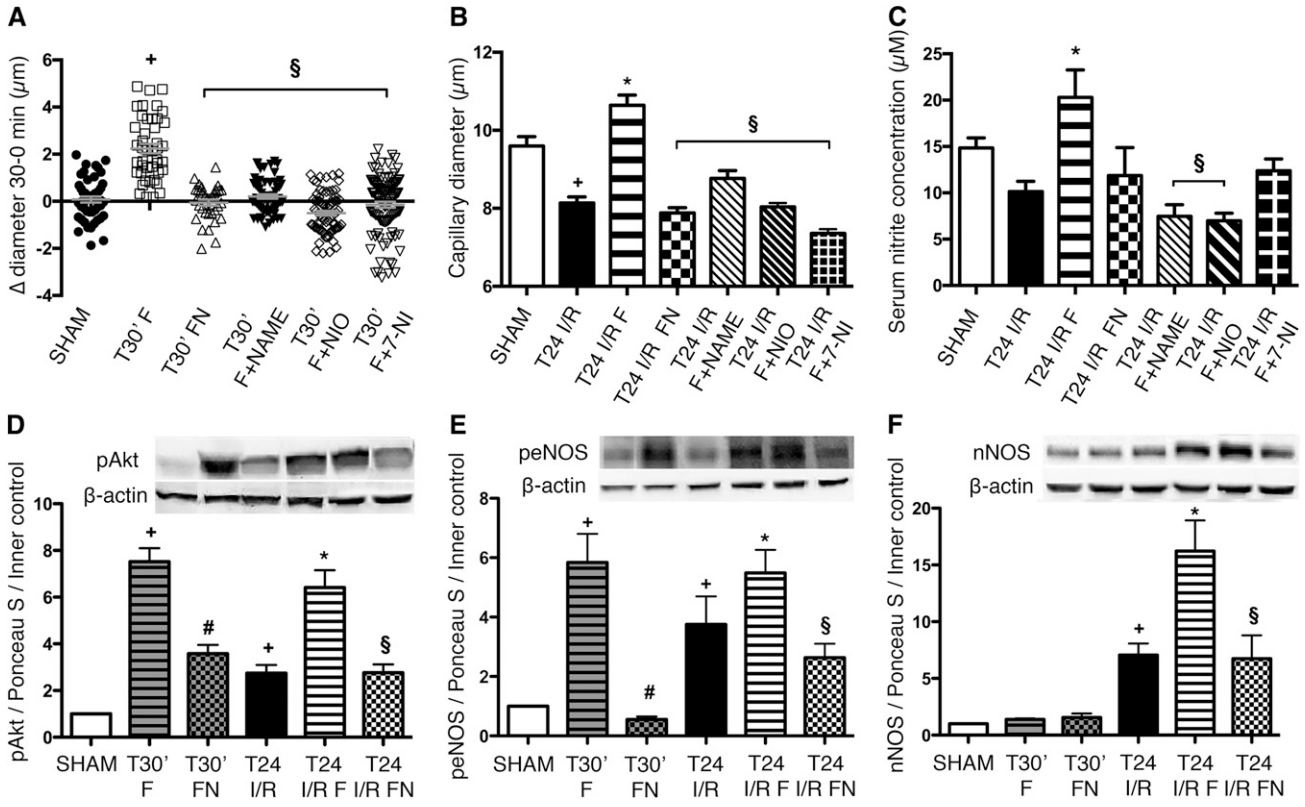

Figure 8. FLU induces S1R–mediated NOS production and vasodilation in the rat kidney. (A) Changes in capillary diameters 30 minutes after FLU (T30′ F), FLU + NE100 (T30′ FN), FLU + nonselective NOS blocker *N*-ω-Nitro-L-arginine methyl ester (T30′ F + NAME), FLU + selective eNOS blocker *N*-5-(1-Iminoethyl)-L-ornithine dihydrochloride (F + NIO), and FLU + selective nNOS blocker 7-Nitroindazole (F + 7-NI) treatment in sham-operated rats. Approximately 150 capillaries per animal. $^{+}P<0.05$ versus sham (n=3 per group); $^{\S}P<0.05$ versus T30′ F (n=3 per group). (B) Capillary diameters after 24 hours of reperfusion. Approximately 150 capillaries per animal. $^{*}P<0.05$ versus T24 I/R (n=3 per group); $^{+}P<0.05$ versus sham (n=3 per group); $^{\S}P<0.05$ versus T24 I/R F (n=3 per group). (C) Serum nitrite concentration of rats after 24 hours of reperfusion. $^{*}P<0.05$ versus T24 I/R (n=6 per group); $^{\S}P<0.05$ versus T24 I/R F (n=6 per group). Immunoblot for renal (D) pAkt (Ser473), (E) peNOS (Ser1177), and (F) nNOS expression in FLU (T30′ F) and FLU + NE100 (T30′ FN) –treated sham–operated rats and after 24 hours of IRI. Representative blots are shown. Bars indicate means±SEMs, and data were analyzed by one-way ANOVA with Bonferroni multiple comparison test. $^{*}P<0.05$ versus T24 I/R (n=5–7 per group); $^{+}P<0.05$ versus sham (n=5–7 per group); $^{\#}P<0.05$ versus T30′ I/R F (n=5–7 per group); $^{\S}P<0.05$ versus T24 I/R F (n=5–7 per group).

Furthermore, various studies showed that FLU is the only SSRI that has no appreciable effect on the norepinephrine system either.[38]

In summary, we, for the first time, provide evidence for the protective role of FLU in renal IRI. Our findings have chalked out a molecular pathway of S1R–mediated renal vasodilation involving S1R translocation, activation of the Akt pathway, and nitrite production. In our rat model, S1R agonist FLU substantially improved postischemic survival and renal function *via* activating S1R-NO signaling in the kidney, which suggests that S1R could be an ideal target to prevent renal IRI.

treatments. Representative blots are shown (n=5 per group). (H) Immunoblot for peNOS (Ser1177) protein level of HK2 cells after various treatments compared with control cells. $^{*}P<0.05$ versus H_2O_2 (n=5–6 per group); $^{+}P<0.05$ versus C (n=5–6 per group); $^{\S}P<0.05$ versus F (n=5–6 per group); $^{\$}P<0.05$ versus H_2O_2 F (n=5–6 per group). Immunoblots for (I) S1R and (J) peNOS expression of S1R knockdown HK2 cells compared with scrambled siRNA–treated negative control (Neg. C) cells. Representative blots are shown. $^{+}P<0.05$ versus Neg.C (n=6 per group). (K) Immunoblot for peNOS protein level of HK2 cells after FLU (F), FLU + NE100 (FN), FLU + AktVIII inhibitor (F + Akt VIII), and FLU + AktIV inhibitor (F + Akt IV) treatment. $^{*}P<0.05$ versus C (n=6 per group); $^{\S}P<0.05$ versus F (n=6 per group). (L) Nitrite production of HK2 cells after FLU and various inhibitor treatments. Bars indicate means±SEMs, and data were analyzed by one-way ANOVA with Bonferroni multiple comparison test. $^{*}P<0.05$ versus C (n=6 per group); $^{\S}P<0.05$ versus F (n=6 per group).

CONCISE METHODS

In Vivo Model

Male Wistar rats weighing 205±15 g (Toxi-Coop Toxicological Research Center, Dunakeszi, Hungary) were housed in standard laboratory cages and allowed free access to food and water. Animal procedures were approved by the Committee on the Care of Laboratory Animals at Semmelweis University (Budapest, Hungary).

Surgical Procedure

General anesthesia was performed by inhalation of isoflurane (3% vol/vol) mixed with air (1 L/min) in an isoflurane vaporizer (Eickemeyer Veterinary Equipment Ltd., Twickenham, United Kingdom). Renal ischemia was accomplished by crossclamping the left renal pedicles for 50 minutes with an atraumatic vascular clamp, and ischemia was visually confirmed. Before the end of the ischemic period, the contralateral kidney was taken out, the clips were removed, and the left kidneys were observed for 5 minutes to ensure reperfusion. Sham animals underwent laparotomy of the same duration without clamping. At predetermined times of reperfusion, blood samples were collected from the abdominal aorta, and the remnant kidneys were harvested, instantly snap frozen in liquid nitrogen, and stored at −80°C or fixed in buffered 4% formalin for additional processing. Plasma chemistry of animals was analyzed using standard autoanalyzer methods by our hospital's research services.

Treatment Protocols

To test the effect of DHEA in the first set of experiments, rats were pretreated first 25 hours and then, 1 hour before the surgical procedure with (*1*) isotonic saline as vehicle, (*2*) 4 mg kg^{-1} body wt DHEA (Sigma-Aldrich, St. Louis, MO), or (*3*) 4 mg kg^{-1} body wt DHEA and 1 mg kg^{-1} body wt NE100 (Tocris Bioscience, Bristol, United Kingdom).

To investigate the effect of FLU in the second set of experiments 30 minutes before the ischemic insult, animals were treated as follows: (*1*) isotonic saline as vehicle, (*2*) 20 mg kg^{-1} body wt FLU (Sigma-Aldrich), or (*3*) 20 mg kg^{-1} body wt FLU and 1 mg kg^{-1} body wt NE100.

In the third set of experiments, to test the NO-mediated effect, the following pretreatment was applied 30 minutes before the ischemic insult: 20 mg kg^{-1} body wt FLU and 10 mg kg^{-1} body wt *N*-ω-Nitro-L-arginine methyl ester (nonselective NOS inhibitor; Sigma-Aldrich) or 20 mg kg^{-1} body wt *N*-5-(1-Iminoethyl)-L-ornithine dihydrochloride (selective eNOS inhibitor),[39] or 25 mg kg^{-1} body wt 7-Nitroindazole (selective nNOS inhibitor).[40]

DHEA was administered subcutaneously; all other substances were administered intraperitoneally.

Experimental Design

In one series, postischemic survival was followed for 7 days (Supplemental Figure 1).

In another series, animals were randomly divided into the following groups: (*1*) sham–operated, vehicle–treated group as controls, (*2*) T30' group that was not subjected to ischemic insult and euthanized or underwent intravital two–photon microscopic analysis 30 minutes after drug pretreatment, (*3*) T2 group that was subjected to ischemia 30 minutes after drug pretreatment and euthanized after 2 hours of reperfusion, and (*4*) T24 group that was subjected to ischemia 30 minutes after drug pretreatment and euthanized or underwent two–photon microscopic analysis after 24 hours of reperfusion.

In Vitro Model

Cell Culture and Treatment

Human proximal tubular epithelial cell line (HK2; American Type Culture Collection, Manassas, VA) were grown in DMEM (Life Sciences, Budapest, Hungary) supplemented with 10% FCS, 1% L-glutamine, and 1% antibiotic, antimycotic solution (100×; Sigma-Aldrich) containing 10,000 IU/ml penicillin, 10 mg/ml streptomycin, and 25 μg/ml Amphotericin B. The cells were incubated at 37°C in 5% CO_2 and 95% air. In all experiments, there was a growth arrest period of 24 hours in serum-free medium before treatment.

In vitro oxidative stress was induced by 400 μM H_2O_2 treatment for 30 minutes. Cells were treated as follows: (*1*) 10 μM FLU (30 minutes before harvest), (*2*) FLU + 3 μM NE100, (*3*) FLU + 10 μM AktVIII inhibitor (AktVIII; 1 hour before harvest), and (*4*) FLU + 2 μM AktIV inhibitor (AktIV; 1 hour before harvest). After treatment, the cells were processed for nitrite measurement.

Before the experiments, the nontoxic dosages of FLU and NE100 were confirmed by methyl-thiazoletetrazolium assay (Roche Diagnostics, Indianapolis, IN) (Supplemental Figure 2).

Cell Viability and Proliferation Assay

Cell viability was determined by methyl-thiazoletetrazolium assay according to the manufacturer's instructions. Cell viability was also assessed by Trypan blue exclusion. Cells were detached with trypsin-EDTA and resuspended in medium diluted 1:1 with Trypan blue solution (Sigma-Aldrich). Live cells from triplicate wells were counted in a Burker chamber.

RNA Interference

All reagents for siRNA were purchased from Invitrogen (Carlsbad, CA). HK2s were transfected with 10 nM S1R-specific siRNA or negative control siRNA using Lipofectamine 2000. Successful transfection with 10 nM fluorescently labeled siRNA was visualized with an Olympus IX81 Fluorescent Microscope (Olympus, Tokyo, Japan). The efficacy of knockdown was determined by Western blot.

Subcellular Protein Fractionation

HK2 cells were treated with either 10 μM FLU or 10 μM FLU and 400 μM H_2O_2. After treatment, the cells were processed for further analysis by the Subcellular Protein Fractionation Kit for Cultured Cells (Thermo Scientific, Budapest, Hungary). The adherent cells were harvested with trypsin-EDTA and separated into cytoplasmic, membrane, soluble nuclear, chromatin-bound nuclear, and cytoskeletal extracts. After fractionating, the different cell extract S1R protein levels were determined by Western blot.

Imaging Techniques

Conventional Histology

Paraffin–embedded, 3-μm kidney sections were stained with PAS and hematoxylin eosin to assess tubular injury. Images were taken with a

Zeiss AxioImager A1 Light Microscope (Carl Zeiss GmbH, Jena, Germany). Tubular injury was evaluated on the basis of a semiquantitative scale as it was previously described.[41] Briefly; each cortical tubule showing epithelial cell necrosis and brush border loss was assigned a score of zero for normal, one for loss of brush border or cell necrosis in <25% of tubular cells, two for cell necrosis in 25%–50% of tubular cells, three for cell necrosis in 50%–75% of tubular cells, and four for cell necrosis in >75% of tubular cells. Two fields of magnification ×200 per animal were examined and averaged in a double-blinded fashion by two different pathologists.

Two-Photon Microscopy

The Femto 2D High Sensitivity Galvanoscanner-Based Two-Photon Microscope System (Femtonics Inc., Budapest, Hungary) was used for intravital two–photon microscopy. Fluorescence excitation is provided by a Mai Tai Mode-Locked Titanium-Sapphire Laser (Spectra-Physics Inc., Irvine, CA) and collected in separate photomultiplier tube detectors to a maximal depth of 100 μm. To inject the mixture of dyes, the rat was anesthetized as described above, and a cannula was placed in the carotid artery; 70-kD Rhodamine dextran (Life Technologies, Carlsbad, CA) was used to label the vasculature, Texas Red (Life Sciences) was used to evaluate the reabsorption capacity and the preservation of the brush border, and Hoechst 33342 (Life Technologies) was used to visualize nuclei.

The changes in capillary diameters were measured continuously in every minute for a 30-minute period, and the differences in diameters between the first, 10th, 20th, and 30th minutes were calculated; approximately 150 capillaries were measured per animal.

Images and data volumes were processed using Matlab software (Femtonics Inc.) and ImageJ software (The National Institutes of Health, Bethesda, MD; http://rsb.info.nih.gov/ij/).

DAB Immunohistochemical Staining

Slides were deparaffinized in xylene, rehydrated in graded ethanol series, and washed in dH_2O. Heat–induced epitope retrieval was performed by boiling the tissue sections in citrate buffer (HISTOLS-Citrate Buffer; Histopathology Ltd., Pecs, Hungary) followed by cooling at room temperature (RT) for 20 minutes. Nonspecific sites were blocked (HISTOLS Background Blocking Protein Solution; Histopathology Ltd.) for 10 minutes at RT. Without washing, the slides were incubated with the primary antibody (Rabbit Anti–S1 Receptor; Thermo Fisher Scientific, Vernon Hills, IL) in 1:50 dilution for 1 hour at RT and repeatedly washed in TBS. Secondary antibody (HISTOLS MR Anti Mouse and Rabbit Detection Systems; Histopathology Ltd.) was applied for 30 minutes at RT followed by repeated washing in TBS. Sections were incubated with 3-amino-9-ethylcarbazol (HISTOLS-Resistant AEC Chromogen/Substrate System; Histopathology Ltd.), washed in dH_2O, and counterstained with hematoxylin or PAS followed by washing in tap water.

Fluorescent Immunohistochemistry

Frozen kidney sections were embedded in Shandon Cryomatrix (Thermo Fisher Scientific) and cut to 5-μm slides. Samples were incubated with the specific rabbit S1R (Invitrogen), goat Akt (Santa Cruz Biotechnology, Santa Cruz, CA), and mouse eNOS (BD Biosciences, San Jose, CA) primary antibodies. After repeated washing, slides were incubated with the specific secondary anti–rabbit Alexa Fluor 568 (Invitrogen), anti–goat Alexa Fluor 647 (Invitrogen), or anti–mouse Alexa Fluor 488 (Invitrogen) conjugates and counterstained with Hoechst 33342 (Life Technologies).

HK2 cells were cultured in tissue culture chambers (Sarstedt Kft., Budapest, Hungary). After repeated washing, the cells were fixed in 4% paraformaldehyde, washed again, and permeabilized with Triton X-100 (Sigma-Aldrich). Cells were incubated with the specific mouse S1R antibody (Santa Cruz Biotechnology). After repeated washing, the chambers were incubated with anti–mouse Alexa Fluor 488 conjugate and counterstained with Hoechst 33342. Appropriate controls were performed, omitting the primary antibody to assure the specificity and avoid autofluorescence. Sections were analyzed with a Zeiss LSM 510 Meta Confocal Laser-Scanning Microscope (Carl Zeiss GmbH) with objectives of magnification ×20 and ×63.

Quantitative RT-PCR

Total RNA was extracted using the RNeasy RNA Isolation Kit (Qiagen, Germantown, MD). Hif-1α, Ngal, Kim-1, and glyceraldehyde-3-phosphate dehydrogenase mRNA expression was determined in duplicate by real–time RT-PCR using SYBR Green I Master Enzyme Mix (Invitrogen) and specific primers (sequences are in Supplemental Table 1). Results were analyzed by the LightCycler 480 SYBR Green I Light Cycler System (Roche Diagnostics). The mRNA expression of Hif-1α, Ngal, and Kim-1 was normalized against mRNA expression of *glyceraldehyde-3-phosphate dehydrogenase* as a housekeeping gene.

Measurement of NO Levels

The total stable oxidation products of NO metabolism (NO_2/NO_3) of serum and HK2 cell homogenates were assessed using Griess Reagent (Promega, Madison, WI). Following the manufacturer's directions, 50 μl samples were incubated with 50–50 μl Griess Reagent (part 1: 1% sulphanilamide; part 2: 0.1% naphthylethylene diamide dihydrochloride and 2% phosphoric acid) at RT. Ten minutes later, the absorbance was measured at 540 nm using a Plate Chameleon V Fluorometer-Luminometer-Photometer Reader (Hidex, Turku, Finland). Relative concentration was calculated on the basis of a sodium nitrite reference curve and expressed in micromolar.

Western Blot Analysis

All reagents for PAGE and Western blot were purchased from Bio-Rad (Hercules, CA). Kidney samples were sonicated and resuspended in lysis buffer. Protein concentration measurement was performed with a detergent–compatible protein assay kit. Samples were electrophoretically resolved on 7.5%, 10%, or 12% polyacrylamide gels and transferred to nitrocellulose membranes. The membranes were incubated with antibodies specific for rat or human S1R (rat: 423300; Invitrogen; human: sc-166392; Santa Cruz Biotechnology), peNOS (Ser1177; 9571; Cell Signaling Technology, Danvers, MA), pAkt (Ser473; 9271; Cell Signaling Technology), and nNOS (sc-5302; Santa Cruz Biotechnology). After repeated washing, the blots were incubated with the corresponding HRP–conjugated secondary antibodies.

Bands of interest were detected using enhanced chemiluminescence detection (GE Healthcare, Waukesha, WI) and quantified by densitometry (VersaDoc; Quantity One Analysis software; Bio-Rad) as integrated OD (IOD) after subtraction of background. IOD was factored for Ponceau red staining as well as β-actin to correct for any variations in total protein loading and internal control. Protein abundance was represented as IOD/Ponceau S/internal control.[42]

Cytometric Bead Array

All reagents and equipment for CBA were purchased from BD Biosciences. Saline–perfused kidney homogenates were measured for TNF-α, IL-1α, IFN-γ, IL-4, and IL-10 peptide levels using appropriate rat CBA Flex Sets according to the manufacturer's protocol. Measurements have been performed using an FACSVerse Flow Cytometer, and data were analyzed using FCAP Array software.

Statistical Analyses

Parametric data are expressed as means$\pm$SEMs, whereas nonparametric data are expressed as medians $\pm$ ranges. Statistical analyses were performed using Prism software (version 5.00; GraphPad Software, La Jolla, CA). Survival studies were assessed by log rank test. Multiple comparisons and possible interactions were evaluated by one-way ANOVA followed by Bonferroni *post hoc* test. For nonparametric data, the Kruskal–Wallis ANOVA on ranks followed by Fisher exacts test was used. P values of <0.05 were considered significant.

ACKNOWLEDGMENTS

The authors are grateful to Prof. Veronika Müller and Dr. Agnes Prokai for their help with surgical procedures and two-photon microscopy. The technical assistance of Maria Bernath and Maria Godo is also highly appreciated.

This study was funded by OTKA K112629, K108688, K100909, K108655, PD105361 and NN114607 grants of the Hungarian Scientific Research Fund and MTA-SE "Lendulet" Research Grant (LP-008/2015) of the Hungarian Academy of Sciences.

DISCLOSURES

None.

REFERENCES

1. Schrier RW, Wang W, Poole B, Mitra A: Acute renal failure: Definitions, diagnosis, pathogenesis, and therapy. *J Clin Invest* 114: 5–14, 2004
2. Himmelfarb J, Ikizler TA: Acute kidney injury: Changing lexicography, definitions, and epidemiology. *Kidney Int* 71: 971–976, 2007
3. Fekete A, Vannay A, Vér A, Rusai K, Müller V, Reusz G, Tulassay T, Szabó AJ: Sex differences in heat shock protein 72 expression and localization in rats following renal ischemia-reperfusion injury. *Am J Physiol Renal Physiol* 291: F806–F811, 2006
4. Müller V, Losonczy G, Heemann U, Vannay A, Fekete A, Reusz G, Tulassay T, Szabó AJ: Sexual dimorphism in renal ischemia-reperfusion injury in rats: Possible role of endothelin. *Kidney Int* 62: 1364–1371, 2002
5. Fekete A, Vannay A, Vér A, Vásárhelyi B, Müller V, Ouyang N, Reusz G, Tulassay T, Szabó AJ: Sex differences in the alterations of Na(+), K(+)-ATPase following ischaemia-reperfusion injury in the rat kidney. *J Physiol* 555: 471–480, 2004
6. Rusai K, Prókai A, Szebeni B, Mészáros K, Fekete A, Szalay B, Vannay Á, Degrell P, Müller V, Tulassay T, Szabó AJ: Gender differences in serum and glucocorticoid regulated kinase-1 (SGK-1) expression during renal ischemia/reperfusion injury. *Cell Physiol Biochem* 27: 727–738, 2011
7. Erdely A, Greenfeld Z, Wagner L, Baylis C: Sexual dimorphism in the aging kidney: Effects on injury and nitric oxide system. *Kidney Int* 63: 1021–1026, 2003
8. Vannay A, Fekete A, Langer R, Tóth T, Sziksz E, Vásárhelyi B, Szabó AJ, Losonczy G, Adori C, Gál A, Tulassay T, Szabó A: Dehydroepiandrosterone pretreatment alters the ischaemia/reperfusion-induced VEGF, IL-1 and IL-6 gene expression in acute renal failure. *Kidney Blood Press Res* 32: 175–184, 2009
9. Liu D, Dillon JS: Dehydroepiandrosterone stimulates nitric oxide release in vascular endothelial cells: Evidence for a cell surface receptor. *Steroids* 69: 279–289, 2004
10. Maurice T, Urani A, Phan VL, Romieu P: The interaction between neuroactive steroids and the sigma1 receptor function: Behavioral consequences and therapeutic opportunities. *Brain Res Brain Res Rev* 37: 116–132, 2001
11. Hellewell SB, Bruce A, Feinstein G, Orringer J, Williams W, Bowen WD: Rat liver and kidney contain high densities of sigma 1 and sigma 2 receptors: Characterization by ligand binding and photoaffinity labeling. *Eur J Pharmacol* 268: 9–18, 1994
12. Pontén F, Gry M, Fagerberg L, Lundberg E, Asplund A, Berglund L, Oksvold P, Björling E, Hober S, Kampf C, Navani S, Nilsson P, Ottosson J, Persson A, Wernérus H, Wester K, Uhlén M: A global view of protein expression in human cells, tissues, and organs. *Mol Syst Biol* 5: 337, 2009
13. Cobos EJ, Entrena JM, Nieto FR, Cendán CM, Del Pozo E: Pharmacology and therapeutic potential of sigma(1) receptor ligands. *Curr Neuropharmacol* 6: 344–366, 2008
14. Bhuiyan MS, Tagashira H, Fukunaga K: Sigma-1 receptor stimulation with fluvoxamine activates Akt-eNOS signaling in the thoracic aorta of ovariectomized rats with abdominal aortic banding. *Eur J Pharmacol* 650: 621–628, 2011
15. Tagashira H, Bhuiyan S, Shioda N, Hasegawa H, Kanai H, Fukunaga K: Sigma1-receptor stimulation with fluvoxamine ameliorates transverse aortic constriction-induced myocardial hypertrophy and dysfunction in mice. *Am J Physiol Heart Circ Physiol* 299: H1535–H1545, 2010
16. Deplanque D, Venna VR, Bordet R: Brain ischemia changes the long term response to antidepressant drugs in mice. *Behav Brain Res* 219: 367–372, 2011
17. Conde E, Alegre L, Blanco-Sánchez I, Sáenz-Morales D, Aguado-Fraile E, Ponte B, Ramos E, Sáiz A, Jiménez C, Ordoñez A, López-Cabrera M, del Peso L, de Landázuri MO, Liaño F, Selgas R, Sanchez-Tomero JA, García-Bermejo ML: Hypoxia inducible factor 1-alpha (HIF-1 alpha) is induced during reperfusion after renal ischemia and is critical for proximal tubule cell survival. *PLoS One* 7: e33258, 2012
18. Bolignano D, Donato V, Coppolino G, Campo S, Buemi A, Lacquaniti A, Buemi M: Neutrophil gelatinase-associated lipocalin (NGAL) as a marker of kidney damage. *Am J Kidney Dis* 52: 595–605, 2008
19. Han WK, Bailly V, Abichandani R, Thadhani R, Bonventre JV: Kidney Injury Molecule-1 (KIM-1): A novel biomarker for human renal proximal tubule injury. *Kidney Int* 62: 237–244, 2002
20. Chertow GM, Burdick E, Honour M, Bonventre JV, Bates DW: Acute kidney injury, mortality, length of stay, and costs in hospitalized patients. *J Am Soc Nephrol* 16: 3365–3370, 2005
21. Smith GL, Vaccarino V, Kosiborod M, Lichtman JH, Cheng S, Watnick SG, Krumholz HM: Worsening renal function: What is a clinically meaningful change in creatinine during hospitalization with heart failure? *J Card Fail* 9: 13–25, 2003

22. Movafagh S, Crook S, Vo K: Regulation of hypoxia-inducible factor-1a by reactive oxygen species: New developments in an old debate. *J Cell Biochem* 116: 696–703, 2015
23. Sun G, Zhou Y, Li H, Guo Y, Shan J, Xia M, Li Y, Li S, Long D, Feng L: Over-expression of microRNA-494 up-regulates hypoxia-inducible factor-1 alpha expression via PI3K/Akt pathway and protects against hypoxia-induced apoptosis. *J Biomed Sci* 20: 100, 2013
24. Hacham M, Argov S, White RM, Segal S, Apte RN: Different patterns of interleukin-1alpha and interleukin-1beta expression in organs of normal young and old mice. *Eur Cytokine Netw* 13: 55–65, 2002
25. Luheshi NM, Kovács KJ, Lopez-Castejon G, Brough D, Denes A: Interleukin-1α expression precedes IL-1β after ischemic brain injury and is localised to areas of focal neuronal loss and penumbral tissues. *J Neuroinflammation* 8: 186, 2011
26. Deng J, Kohda Y, Chiao H, Wang Y, Hu X, Hewitt SM, Miyaji T, McLeroy P, Nibhanupudy B, Li S, Star RA: Interleukin-10 inhibits ischemic and cisplatin-induced acute renal injury. *Kidney Int* 60: 2118–2128, 2001
27. Yap SC, Lee HT: Acute kidney injury and extrarenal organ dysfunction: New concepts and experimental evidence. *Anesthesiology* 116: 1139–1148, 2012
28. Allahtavakoli M, Jarrott B: Sigma-1 receptor ligand PRE-084 reduced infarct volume, neurological deficits, pro-inflammatory cytokines and enhanced anti-inflammatory cytokines after embolic stroke in rats. *Brain Res Bull* 85: 219–224, 2011
29. Hayashi T, Su TP: Sigma-1 receptor chaperones at the ER-mitochondrion interface regulate Ca(2+) signaling and cell survival. *Cell* 131: 596–610, 2007
30. Hayashi T, Su TP: Intracellular dynamics of sigma-1 receptors (sigma(1) binding sites) in NG108-15 cells. *J Pharmacol Exp Ther* 306: 726–733, 2003
31. Mori T, Hayashi T, Hayashi E, Su TP: Sigma-1 receptor chaperone at the ER-mitochondrion interface mediates the mitochondrion-ER-nucleus signaling for cellular survival. *PLoS One* 8: e76941, 2013
32. Chaigneau E, Oheim M, Audinat E, Charpak S: Two-photon imaging of capillary blood flow in olfactory bulb glomeruli. *Proc Natl Acad Sci U S A* 100: 13081–13086, 2003
33. Crawford C, Kennedy-Lydon T, Sprott C, Desai T, Sawbridge L, Munday J, Unwin RJ, Wildman SS, Peppiatt-Wildman CM: An intact kidney slice model to investigate vasa recta properties and function in situ. *Nephron, Physiol* 120: 17–31, 2012
34. Smith C, Merchant M, Fekete A, Nyugen HL, Oh P, Tain YL, Klein JB, Baylis C: Splice variants of neuronal nitric oxide synthase are present in the rat kidney. *Nephrol Dial Transplant* 24: 1422–1428, 2009
35. Shoskes DA, Xie Y, Gonzalez-Cadavid NF: Nitric oxide synthase activity in renal ischemia-reperfusion injury in the rat: Implications for renal transplantation. *Transplantation* 63: 495–500, 1997
36. Szabo AJ, Wagner L, Erdely A, Lau K, Baylis C: Renal neuronal nitric oxide synthase protein expression as a marker of renal injury. *Kidney Int* 64: 1765–1771, 2003
37. Nishimura T, Ishima T, Iyo M, Hashimoto K: Potentiation of nerve growth factor-induced neurite outgrowth by fluvoxamine: Role of sigma-1 receptors, IP3 receptors and cellular signaling pathways. *PLoS One* 3: e2558, 2008
38. Miller HL, Ekstrom RD, Mason GA, Lydiard RB, Golden RN: Noradrenergic function and clinical outcome in antidepressant pharmacotherapy. *Neuropsychopharmacology* 24: 617–623, 2001
39. Chen W, Qi J, Feng F, Wang MD, Bao G, Wang T, Xiang M, Xie WF: Neuroprotective effect of allicin against traumatic brain injury via Akt/endothelial nitric oxide synthase pathway-mediated anti-inflammatory and anti-oxidative activities. *Neurochem Int* 68: 28–37, 2014
40. Hsu YC, Chang YC, Lin YC, Sze CI, Huang CC, Ho CJ: Cerebral microvascular damage occurs early after hypoxia-ischemia via nNOS activation in the neonatal brain. *J Cerebral Blood Flow Metab* 34: 668–676, 2014
41. Rong S, Park JK, Kirsch T, Yagita H, Akiba H, Boenisch O, Haller H, Najafian N, Habicht A: The TIM-1:TIM-4 pathway enhances renal ischemia-reperfusion injury. *J Am Soc Nephrol* 22: 484–495, 2011
42. Romero-Calvo I, Ocón B, Martínez-Moya P, Suárez MD, Zarzuelo A, Martínez-Augustin O, de Medina FS: Reversible Ponceau staining as a loading control alternative to actin in Western blots. *Anal Biochem* 401: 318–320, 2010

This article contains supplemental material online at http://jasn.asnjournals.org/lookup/suppl/doi:10.1681/ASN.2015070772/-/DCSupplemental.